CONTRAST MEDIA & MOLECULAR IMAGING

Received: 30 September 2014, Revised: 17 March 2015, Accepted: 01 April 2015, Published online in Wiley Online Library: 27 May 2015

(wileyonlinelibrary.com) DOI: 10.1002/cmmi.1644

Optoacoustic imaging enabled biodistribution study of cationic polymeric biodegradable nanoparticles

Susana P. Egusquiaguirre[a,b], Nicolas Beziere[c], José Luís Pedraz[a,b], Rosa M. Hernández[a,b], Vasilis Ntziachristos[c]*† and Manuela Igartua[a,b]*†

Nanosized contrast agents for molecular imaging have attracted widespread interest for diagnostic applications with high resolution in medicine. However, many solid nanoparticles exhibit a great potential to induce toxicity, hindering their use for clinical applications. On the other hand, near-infrared (NIR) dyes have also been used for extensive biological applications, but show some limitations due to their poor aqueous stability, tendency to aggregation and rapid elimination from the body. An alternative proposed in this work to overcome these limitations is the use of NIR dye-loaded nanoparticles. Here we introduce nanoparticles constructed with poly(D,L-lactide-co-glycolic acid) (PLGA), a biodegradable and biocompatible polymer widely used for biomedical applications, attached to the polycation polyethyleneimine (PEI) to obtain positively charged nanoparticles. The *in vivo* biodistribution of the cationic PEI–PLGA nanoparticles was investigated after administration through three different routes (intravenous, intraperitoneal and subcutaneous) using multispectral optoacoustic tomography (MSOT). The prepared nanoparticles exhibited good colloidal stability and adequate optical properties for optoacoustic imaging. The *in vivo* biodistribution assays indicated a strong accumulation of the particles in the liver and spleen, and retention in these organs for at least 24 h. Therefore, these nanoparticles could find promising applications in MSOT due to a sharp and characteristic optoacoustic spectrum and high optoacoustic signal generation, and become a promising building block for theranostic strategies. Copyright © 2015 John Wiley & Sons, Ltd.

Additional supporting information may be found in the online version of this article at the publisher's web site.

Keywords: biodistribution; cationic nanoparticles; imaging; MSOT; optoacoustic; nanoparticles

1. INTRODUCTION

Over the last decade, molecular imaging in biological systems has attracted great attention as a promising strategy used in health-care for monitoring processes at cellular and subcellular levels, as well as the diagnosis and tracking of the progress of pathologies, and eventually their treatment. Therefore, it is important to develop suitable imaging platforms that could be used as contrast agents to trace these issues *in vivo*.

Optical imaging techniques have been widely used to attain these purposes, although the low imaging depth, due to photon scattering, limits their use *in vivo*. However, multispectral optoacoustic tomography (MSOT) (1) is able to overcome these shortcomings, and its outstanding properties, including high resolution, high penetration depth and detection sensitivity, as well as real-time monitoring and the use of non-ionizing radiation, qualify it as the ideal modality for preclinical and clinical translation investigations. While providing an elegant way to monitor pathophysiological parameters based on light absorbance of either endogeneous (hemoglobin, melanin, …) or exogenous contrast agents, it can also enable observation of the behavior of nanosized compounds such as drug delivery platforms *in vivo* and in real time, provided they display adequate light absorbing properties.

Until now, a broad variety of nanoparticles have been studied for enhancing contrast in optoacoustic imaging, the most common being gold nanorods (2,3) and single-walled carbon nanotubes (SWNTs) (4), with a high molar extinction (absorption) coefficient and photostability, making them excellent candidates as contrast agents for optoacoustics (5). However, even though many drug delivery platforms based on this type of nanoparticle are currently being developed (6), issues related to safety and

* *Correspondence to: V. Ntziachristos, Institute for Biological and Medical Imaging, Technische Universität München and Helmholtz Zentrum München, Ingolstädter Landstraße 1, 85764 Neuherberg, Germany. E-mail: v.ntziachristos@helmholtz-muenchen.de*
M. Igartua, NanoBioCel Group, Laboratory of Pharmaceutics, School of Pharmacy, University of the Basque Country (UPV/EHU), Paseo de la Universidad 7, 01006 Vitoria-Gasteiz, Spain. E-mail: manoli.igartua@ehu.es

† *M. Igartua (manoli.igartua@ehu.es) and V. Ntziachristos (v.ntziachristos@helmholtz-muenchen.de) equally share credit for senior authorship.*

a *S. P. Egusquiaguirre, J. L. Pedraz, R. M. Hernández, M. Igartua*
NanoBioCel Group, Laboratory of Pharmaceutics, School of Pharmacy, University of the Basque Country (UPV/EHU), Paseo de la Universidad 7, 01006, Vitoria-Gasteiz, Spain

b *S. P. Egusquiaguirre, J. L. Pedraz, R. M. Hernández, M. Igartua*
Biomedical Research Networking Center in Bioengineering, Biomaterials and Nanomedicine (CIBER-BBN), Paseo de la Universidad 7, 01006, Vitoria-Gasteiz, Spain

c *N. Beziere, V. Ntziachristos*
Institute for Biological and Medical Imaging, Technische Universität München and Helmholtz Zentrum München, Ingolstädter Landstraße 1, 85764, Neuherberg, Munich, Germany

toxicity hinder the diffusion of their use to the clinic. The optical properties displayed by the nanoparticles play a crucial role in their suitability for optoacoustic imaging: indeed, a strong detectable signal in the near-infrared (NIR) region (700–900 nm, also called the NIR window) is paramount, as low tissue absorption and little NIR autofluorescence is generated in this window (7). Other biocompatible nanoparticles can be used as drug carriers, but do not possess adequate optical properties for accurate optoacoustic imaging. Biodegradable polymer poly(lactic-co-glycolic acid) (PLGA) particles are shown to exhibit excellent properties for biomedicine (8), being FDA and EMA approved (9). After administration, PLGA can undergo hydrolysis in the organism, yielding lactic acid and glycolic acid, naturally present in the body and easily removed through physiological pathways and devoid of toxicity. Additionally, PLGA nanoparticles can be readily functionalized through their carboxylic functional groups on their surface, potentially enabling vectorization, specific targeting, labeling for imaging applications and stealth or improvement of interactions with biological materials through easily accessible synthetic chemistry (10). For this reason, they represent an extremely promising class of nanocarriers for drug delivery applications. However, they do not possess the optical properties required for efficient optoacoustic imaging and thus require optical labeling in order to generate contrast in the imaging modality. Alone, NIR contrast agents usually display poor stability, tendency to aggregation, predisposition to photobleaching, lack of targeting specificity and fast removal from the body. However, these properties of organic dyes can be significantly altered when used as photolabels. Their encapsulation in nanoparticles allows for a much better control of their pharmacokinetic profile through functionalization, such as pegylation of the surface for increased circulation time, surface modification with polycations for enhanced cellular uptake, or peptide grafting (with cell penetrating peptides or specific ligands) to obtain active and selective targeting strategies (11). Thus, labeling nanocarriers using optical contrast agents allows direct imaging of the behavior of the drug delivery vehicle *in vivo*, and the influence its chemical structure and external functionalization has on its pharmacokinetic profile. Furthermore, the potency of PLGA nanoprobes labeled with NIR dyes used as promising optoacoustic contrast agents has been previously described (12,13); however, in these studies no *in vivo* tests were performed. Very recently, Wang *et al*. published folate receptor targeted, indocyanine green dye doped PLGA lipid nanoparticles (FA–ICG–PLGA-lipid NPs) for optoacoustic molecular imaging of breast carcinoma, demonstrating the great potential for clinical translation of this approach (14).

Taking all this into account, in this study we have chosen to investigate the fate of the PLGA particles in a rodent model using optoacoustic imaging, enabled by grafting an NIR fluorescent dye (DiR, 1,1′-dioctadecyltetramethyl indotricarbocyanine iodide). As the surface charge of the particles plays an important role in their interactions with cells, we opted for an additional cationic polymer polyethyleneimine (PEI) functionalization of their surface to increase their potential cellular uptake, as was previously reported by our group (15). By using three different administration routes (intraperitoneal, intravenous and subcutaneous), we show that the stability of the dye loading of the nanoparticles allows for efficient tracking in real time and *in vivo* of the behavior of the probe in healthy animal in MSOT, and validate the model for further theranostic studies.

2. MATERIALS AND METHODS

2.1. Materials

The polymer poly(D,L-lactide-co-glycolide) (PLGA, RESOMER RG® 503) 50:50 (lactic/glycolic, %), with a molecular weight (MW) of 33.9 kDa and an intrinsic viscosity of 0.32–0.4 dL/g, was purchased from Boehringer Ingelheim (Ingelheim, Germany). Dichloromethane (DCM, HPLC grade) as the organic solvent, isopropanol, and polyethylene glycol 400 (PEG 400) were acquired from Panreac (Barcelona, Spain). The surfactant used in the emulsification process was poly(vinyl alcohol) (PVA, with an average MW of 30–70 kDa, 87–90% hydrolysis degree), as well as polyethyleneimine (PEI, with an MW of 25 kDa, branched), and D-trehalose (TRH, with an MW of 378.33 g/mol) were obtained from Sigma-Aldrich (Barcelona, Spain). Phosphate buffered saline (PBS) and 1,1′-dioctadecyltetramethyl indotricarbocyanine iodide (DiR) were obtained from Invitrogen, Life Technologies (Germany). All other chemicals and reagents were of analytical grade and purchased from local suppliers.

2.2. Methods

2.2.1. *Preparation of biodegradable nanoparticles*

Cationic PEI–PLGA nanoparticles were elaborated by a previously developed double-emulsion solvent evaporation technique (16) and were fluorescently labeled with the NIR organic dye DiR (Fig. 1). Briefly, 5% (w/v) of PLGA, with 1.3% (w/w) of PEI as the polycation, and 0.5 mg/mL of DiR were first dissolved in the organic solvent (dichloromethane, DCM) and, while sonicating

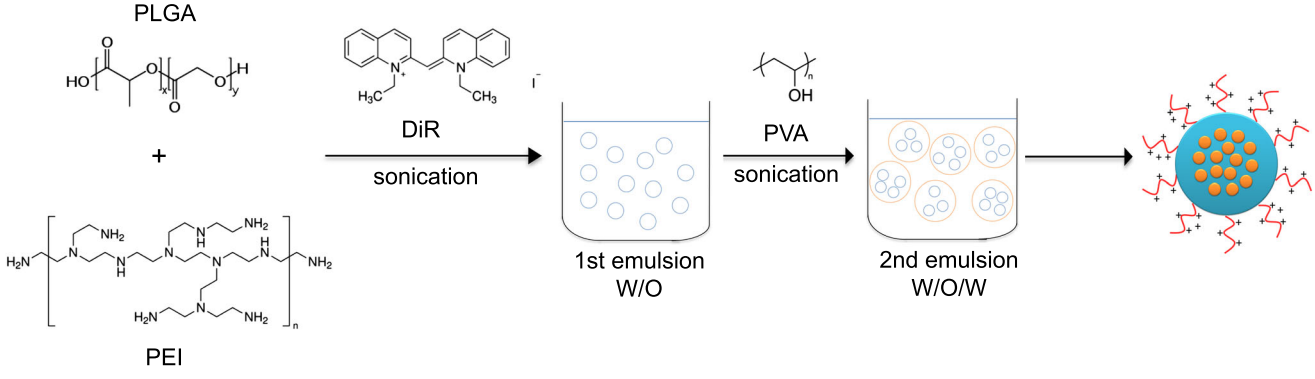

Figure 1. Schematic representation of the process of elaboration of DiR-loaded PEI–PLGA nanoparticles by the double-emulsion solvent evaporation technique.

in an ice bath for 30 s with ultrasound using a sonicator (Branson Ultrasonic Sonifier® 250), an aqueous solution of PEG 400 (2.5% (v/v)) was incorporated to form an oil-in-water emulsion. This first emulsion was then rapidly poured into another aqueous solution of PVA (polyvinyl alcohol, 5% (w/v)) as the emulsifier and was again sonicated for another 60 s to form the double emulsion (W/O/W). Finally, the obtained double emulsion was added to an alcoholic aqueous solution of IPA (isopropanol, 2% (v/v)) and stirred for 2 h in order to favor the organic solvent removal by evaporation. The obtained nanoparticles were collected by ultracentrifugation (25 000 *g*, 15 min, 4 °C, Sigma 3-30 K), and washed three times with water to remove the surfactant.

2.2.2. *Physicochemical characterization of nanoparticles*

A Zetasizer Nano ZS apparatus (Malvern Instruments, UK) was used to determine the mean nanoparticle size (*Z*-average), polydispersity index (PDI) and zeta potential. The samples were re-dispersed and diluted to a suitable density in distilled water at 25 °C. Mean values of three determinations for each sample were obtained and reported.

2.2.3. *Optical properties and stability of the nanoparticles*

2.2.3.1. Spectrometer measurements. An absorption spectrum from each nanoparticle formulation used was recorded on an Ocean Optics CUV-UV + USB2000 spectrometer, and processed with SpectraSuite (Ocean Optics, Ostfildern, Germany).

2.2.3.2. Fluorescence determination. The fluorescence of the nanoparticle formulation was determined using a SpectraMax M2 microplate reader (Molecular Devices, Sunnyvale, CA, USA) using a 96-well culture plate.

2.2.3.3. Dye release. In order to investigate if the dye would be released from the nanoparticles once administered to mice, 2 mg of nanoparticles were incubated for 24 h in 1 mL PBS. After that time, the suspension of the nanoparticles was filtered using a centrifugal filter with a 100 kDa cutoff (Amicon Ultra, Merck Millipore©, Darmstadt, Germany) and centrifuged at 20 000 *g* for 5 min at 4 °C (5424R centrifuge, Eppendorf, Hamburg, Germany). The absorbances of the nanoparticle suspension prior to filtration and the filtrate were measured and compared.

2.2.4. *Optoacoustic imaging procedure and processing*

All MSOT measurements were performed in a custom-built real time optoacoustic imaging system adapted from a previously described experiment (3). Briefly, a *Q*-switched Nd:YAG laser (Phocus, OPOTEK, Carlsbad, CA, USA) provided the optical excitation, with a pulse duration of around 10 ns, a repetition rate of 10 Hz and a tunable range of 680–980 nm. A fiber bundle split into 10 output arms was used to achieve homogeneous delivery of light to the sample. The detection and record of emitted ultrasound waves was obtained by means of a 256 element transducer array cylindrically focused and having a central frequency of 5 MHz, allowing acquisition of transverse plane images. A moving stage enabled the imaging of different planes by the static illumination and detection devices. Measurements were executed in a temperature controlled water bath (34 °C) for acoustic coupling, and to keep the sample dry a clear polyethylene membrane attached to the sample holder was employed.

2.2.5. *Phantom experiments*

In order to verify optoacoustic detection of the DiR nanoparticles, a suspension of the nanoparticle formulation was placed in a cylindrical, light-scattering phantom of 2 cm in diameter, which were assembled using a gel made from distilled water containing agar for jellification (1.3% w/w) and an Intralipid 20% emulsion for light diffusion (6% v/v). This way, a gel with a reduced scattering coefficient of $\mu_s' \approx 10\,cm^{-1}$ was obtained. The sample suspension of nanoparticles was placed into a tube of approximately 3 mm diameter, and was inserted in the middle of the phantom, along with an ink straw having an optical density of 0.2 in order to provide a reference to rule out any system misbehavior *in situ* during the acquisition. Imaging was performed using 30 averages per illumination wavelength, from 680 to 900 nm in steps of 2 nm. The optoacoustic signal strength was derived from a region of interest analysis, using the average signal value measured inside of the sample straw.

2.2.6. *Animal care*

In vivo studies were conducted with CD-1 mice in compliance with the Helmholtz Zentrum München animal care guidelines. All procedures involving animals and their care were performed in full agreement with the institutional guidelines, and under the approval protocol from the government of Upper Bavaria (reference 55.2.1.54-2632-102-11).

2.2.7. *In vivo experiments*

For the imaging experiments, a concentration of DiR-loaded nanoparticles (2 mg of nanoparticles/mL PBS pH 7.4), with an optical density of 1.8, were administered. The nanoparticles were resuspended in the corresponding volume of PBS pH 7.4 according to the administration route, and were injected in the tail vein of anesthetized animals using 2% isoflurane in oxygen for the intravenous administration (injection volume of 200 μL), in the abdominal cavity of the mouse for the intraperitoneal administration (injection volume of 1000 μL), and in the epidermal tissue in the neck of the mouse for the subcutaneous administration (injection volume of 500 μL).

Animals were imaged under anesthesia at 1.5% isoflurane in oxygen throughout the acquisitions, and the body temperature was maintained at 34 °C. Imaging of the animals ($n = 3$) was performed roughly from hips to the thorax using a 0.5 mm steps. After the administration of the nanoparticle suspension, whole body optoacoustic images were recorded with transversal slides at various time points, ranging from 1 h to 5 h to 24 h post-injection. Data acquisition was performed using 30 averages per illumination wavelength, which were as follows: 710, 740, 770, 800, 830 and 860 nm. This resulted in an acquisition time of around 20 min. Animals were sacrificed by ketamine and xylazine overdose after the last imaging time point and stored at −80 °C for further analysis.

2.2.8. *Image processing and signal quantification*

Data processing was performed using the commercial software developed by iThera Medicals (Munich, Germany), where model based image reconstruction is performed on the raw data followed by spectral unmixing, based on spectral fitting by the least square method (1,17).

For the optoacoustic signal quantification, ImageJ software was employed and the mean pixel intensity values of each image were obtained.

2.2.9. Ex vivo tissue imaging/cryosectioning with fluorescence image acquisition

Cryosectioning and epifluorescence imaging were performed using a Leica cryoslicer (CM 1950, Leica Microsystems, Wetzlar, Germany), fitted with a fluorescence imaging system (Sarantopoulos, 2010), with excitation at 740 nm and emission captured with a 780 long pass filter. Sequential slice images were recorded at 250 μm intervals, in the same orientation (transversal plane) and at the same scale as MSOT, showing both anatomy (color) and nanoparticle distribution near-infrared fluorescence (NIRF).

3. RESULTS AND DISCUSSION

3.1. Physicochemical characterization of nanoparticles

The water-in-oil-in-water ($W_1/O/W_2$) double-emulsion solvent evaporation method is mostly preferred in producing nanoparticles, so we prepared the cationic nanoparticles by means of this technique (18). Once achieved, these nanoparticles were characterized by particle size and zeta potential, presenting a mean diameter around 200 nm and a low PDI (<0.2), with a monomodal size distribution. As expected, the external capping of PLGA nanoparticles with PEI resulted in a positive surface charge (+40 mV), clearly confirming the successful attachment of PEI.

3.2. Optical properties and stability of the nanoparticles

Since the toxicity profile of PEI–PLGA particles has been previously reported by our group (15), our next goal was to study the potency of the DiR-loaded PEI–PLGA as an optoacoustic contrastagents *in vitro*. First of all, the absorbance spectra of DiR-loaded PEI–PLGA nanoparticles were obtained from spectrophotometer measurements, and then their optoacoustic properties were investigated in the MSOT imaging system. Figure 2(A) depicts the nanoparticle absorbance spectrum and the optoacoustic signal (OAS) at the corresponding wavelengths acquired during phantom experiments with DiR-loaded PEI–PLGA nanoparticles. As can be observed, the absorbance peak of the nanoparticle suspension obtained at 780 nm and the optoacoustic spectrum closely coincide, confirming that the studied formulation can be identified in the optoacoustic system. Figure 2(B) shows that the fluorescent properties of DiR are conserved after encapsulation within the nanoparticle, confirming correct loading.

To evaluate the loading stability of DiR in the PLGA particles, the nanoconstruct underwent a 24 h incubation time in PBS. After centrifugal filtration, absorbance measurements of the filtrate were made. The absence of detectable absorbance in the filtrate shown in Fig. 2(C) clearly indicates the correct incorporation of the dye inside of the particle and that the dye would not be released from the nanoparticles under those conditions. Figure 2(D) represents an image of the phantom containing the samples (nanoparticles and ink), and Fig. 2(E) shows an optoacoustic image of the phantom with the samples.

According to these results, we can confirm that the stage is set for the *in vivo* experiments, and therefore we proceeded to address the biodistribution of the nanoparticles after their injection through the different routes of administration.

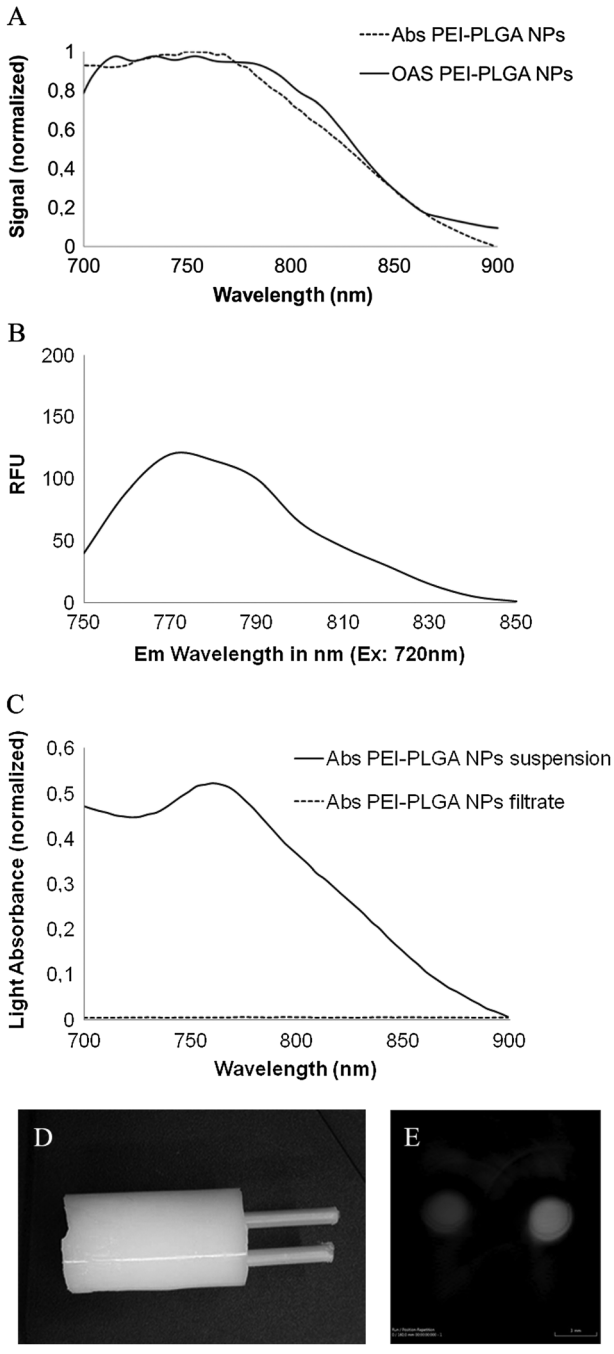

Figure 2. Phantom study of DiR-loaded PEI–PLGA nanoparticles as optoacoustic imaging contract agents. (A) OAS and light absorbance (Abs) comparison of PEI–PLGA nanoparticles, (B) fluorescence determination, and (C) light absorbance comparison of nanoparticle re-suspension and filtrate after centrifugation. (D) Photograph of the agar phantom setup with protruding straws containing samples and (E) resulting multispectral optoacoustic image after spectral identification of DiR-loaded PEI–PLGA particles and India ink acquired at 800 nm.

3.3. Biodistribution studies of nanoparticles

For the animal studies, the same MSOT system as in the phantom experiments was used to investigate the *in vivo* time-dependent distribution of the nanoparticles and their eventual accumulation *in vivo* in CD-1 mice. Optoacoustic images were acquired before and 1 h, 5 h and 24 h after DiR-loaded PEI–PLGA

nanoparticle administration ($n = 3$), through three different routes of administration: intravenous, intraperitoneal and subcutaneous.

First, the nanoparticles (0.4 mg of nanoparticles in 200 μL PBS pH 7.4 per mouse) were injected intravenously into CD-1 mice through the tail vein. The second route of administration tested was the intraperitoneal, in which the nanoparticles (2 mg of nanoparticles in 1000 μL PBS pH 7.4 per mouse) were injected intraperitoneally into the abdomen of the mice. The third route of administration used was the subcutaneous, in which the

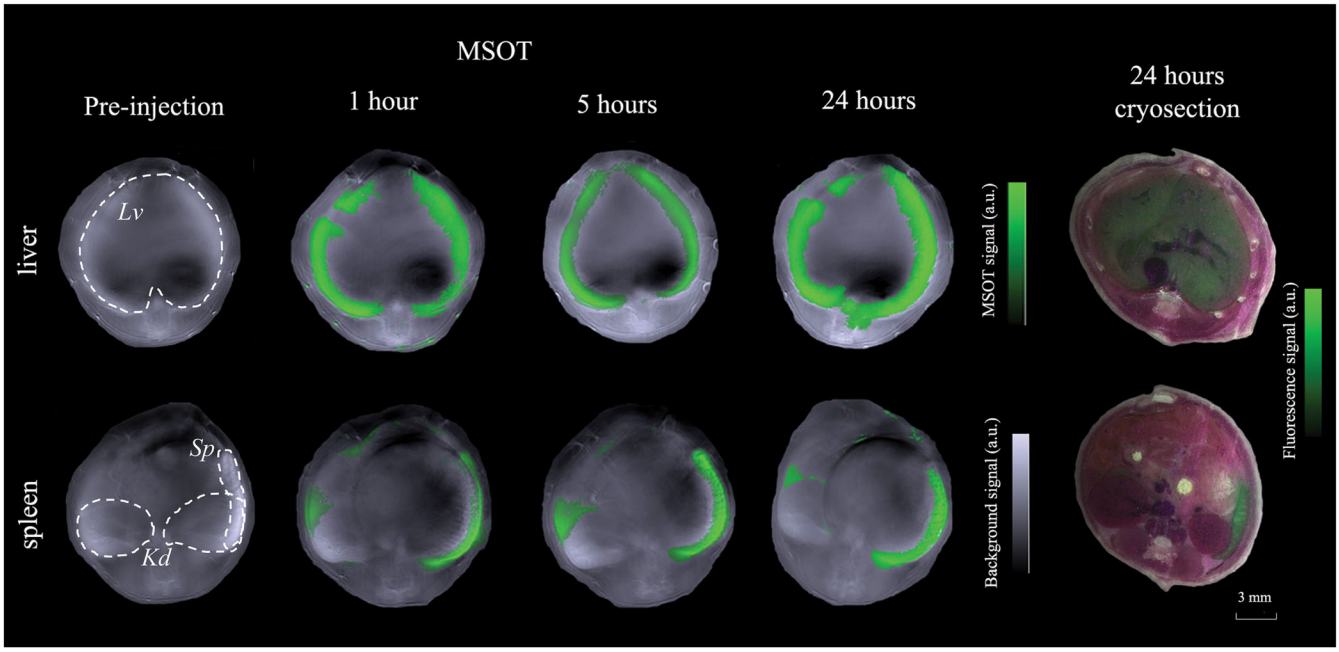

Figure 3. *In vivo* MSOT optoacoustic transverse slice images of healthy CD-1 mice, taken at 800 nm, before (pre-injection) and 1 h, 5 h and 24 h after the injection of DiR-loaded PEI–PLGA nanoparticles through intravenous administration, showing the liver (Lv), spleen (Sp) and kidneys (Kd). The green overlay on the left hand side represents the optoacoustic signals of the PEI–PLGA nanoparticles on the single wavelength optoacoustic signal. Corresponding *ex vivo* cryosectioning transverse slice images at 24 h are presented on the right hand side, where the fluorescence signal of the same particles is overlaid on a color photograph.

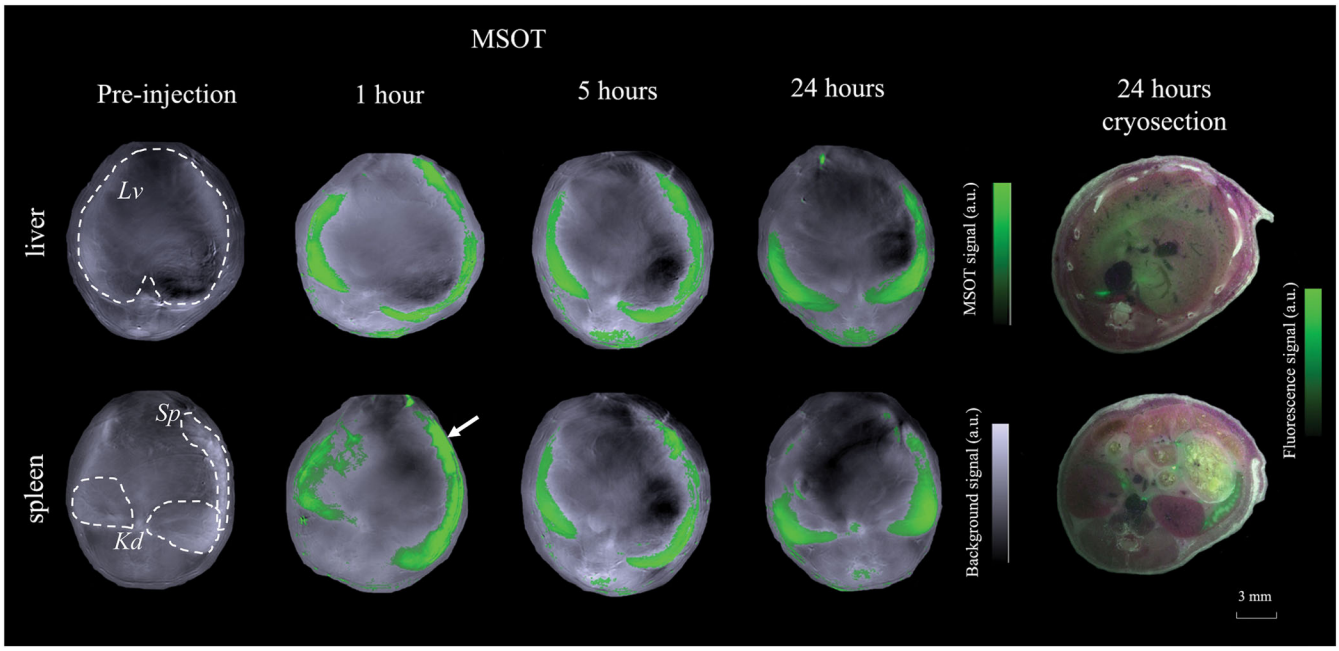

Figure 4. *In vivo* MSOT optoacoustic transverse slice images of healthy CD-1 mice, taken at 800 nm, before (pre-injection) and 1 h, 5 h and 24 h after the injection of DiR-loaded PEI–PLGA nanoparticles through intraperitoneal administration showing the liver (Lv), spleen (Sp) and kidneys (Kd). The green overlay on the left hand side represents the optoacoustic signals of the PEI–PLGA nanoparticles on the single wavelength optoacoustic signal. Corresponding *ex vivo* cryosectioning transverse slice images at 24 h are presented on the right hand side, where the fluorescence signal of the same particles is overlaid on a color photograph. (Arrow: injection site.)

nanoparticles (1 mg of nanoparticles in 500 μL PBS pH 7.4 per mouse) were injected subcutaneously into the epidermal tissue in the neck of the mice.

Figures 3 and 4 compare the biodistribution of positively surface charged DiR-loaded PEI–PLGA nanoparticles following intravenous and intraperitoneal administration, respectively.

As can be seen in Fig. 3, after intravenous administration of PEI–PLGA nanoparticles, the optoacoustic signal was detected in the liver and in the spleen as early as 1 h after injection, exhibiting an impressive contrast, and suggesting the *in vivo* stability and tissue retention of the nanoplatform. This signal was diminished with time, indicating the clearance of the probe. Unfortunately, no signal was observed in any other organs (Supplementary Fig. 1). The equivalent *ex vivo* tissue cryosection from the same animal sacrificed at 24 h shows a green overlay of the fluorescent signal corresponding to the nanoparticles, displaying in both images the signal from the particles in the liver and spleen, matching with the nanoparticle signal observed in the MSOT images.

The intraperitoneal administration of DiR-loaded PEI–PLGA nanoparticles is presented in Fig. 4, where the optoacoustic signals were located mainly at the site of administration as well as in liver and spleen 1 h after injection. At the 5 h time point these nanoparticles exhibited a maximum optoacoustic signal within the liver and spleen, which was gradually decreased with time (24 h post-administration), although it was still detectable in these two organs. However, as before, nothing could be seen within other organs (Supplementary Fig. 1). In the *ex vivo* cryosection from the same animal sacrificed at the 24 h time point, the signal from the nanoparticles (green overlay) can be observed mainly in the liver, and some particles are still seen at the site of administration, correlating with the MSOT images obtained 24 h post-administration of the probe.

As can be appreciated in Figs. 3 and 4, the fluorescent signal from the nanoparticles in the liver cryosection comes from the whole organ, while in the case of the MSOT images the optoacoustic signal from the nanoparticles in the liver is located at the borders of the organ. This phenomenon, which is caused by the penetration of light in tissue and appears when there is a high absorbance, is called the 'fluence problem'. The animal is illuminated from the outside and the light is absorbed on the way, thereby providing more signal close to the surface than in deeper tissues, where the light cannot reach anymore. In the cryoslicer this effect does not occur because the illumination is direct and homogeneous on the surface of each slice.

The quantification results of the optoacoustic signal in the liver and spleen after intravenous or intraperitoneal administration are presented in Fig. 5.

Finally, the optoacoustic signals from the nanoparticles when these were subcutaneously administered were all located at the site of injection, and no detectable signal was recorded in any organ (Supplementary Fig. 2).

After biodistribution studies of cationic DiR-loaded PEI–PLGA nanoparticles, visualization of the behavior of the dye, DiR, after intravenous injection was performed. Images were acquired 5 min and 1 h after injection. It was observed that the dye not encapsulated went directly to the liver and kidneys as early as 5 min post-administration. However, after 1 h it started to disappear from the liver and could mostly be found within the kidneys, confirming the renal excretion pathway. These images showcase the rapid delivery and elimination of the free DiR *in vivo* in MSOT (Supplementary Fig. 3).

A

OAS (mean pixel intensity)

	IV		IP	
	LIVER	SPLEEN	LIVER	SPLEEN
1h	256.30	281.69	226.79	172.02
5h	242.50	249.88	239.98	389.27
24h	178.76	243.83	175.88	275.14

B

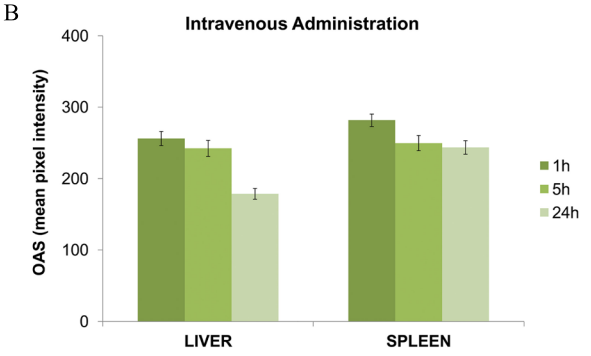

C

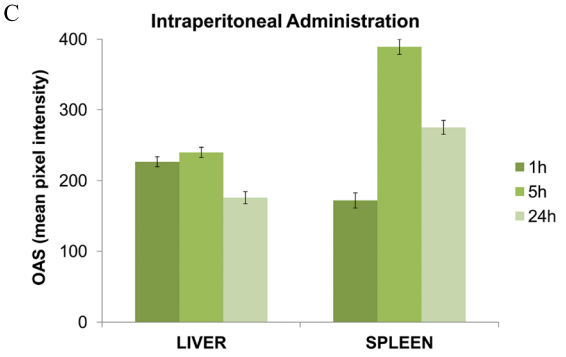

Figure 5. Mean pixel intensity of the OAS in the liver and spleen at 1 h, 5 h and 24 h after intravenous (IV) or intraperitoneal (IP) administration of DiR–PEI–PLGA nanoparticles.

According to the obtained results, the optoacoustic signal remaining high for 24 h after the administration of the cationic biodegradable nanoparticles, indicating a relatively constant number of nanoparticles accumulated in these two organs, could be attributed to their suitable uniform size, of about 200 nm, and a good colloidal stability. Therefore, the biodistribution data for these two routes of administration demonstrate that there seems to be no significant difference in the organ distribution when injecting the nanoparticles through any of the routes studied. In contrast, the free dye is rapidly delivered to the kidneys and cleared from the body through the renal system, as has been previously reported (19), hindering its use as a contrast agent, since longer periods of time in the body would be needed to be able to monitor the progress of diseases and track the delivery of therapeutic agents in real time. These results suggest that the tracking of DiR-labelled cationic biodegradable nanoparticles could be used as an efficient theranostic approach, allowing for tracking in real time of the biodistribution of the nanocarriers *in vivo*.

4. CONCLUSIONS

In the present work, the successfully developed cationic PEI–PLGA nanoparticles encapsulating DiR have demonstrated excellent multispectral optical properties, and their optoacoustic efficiency was found to be significantly better when compared with the

dye administered alone, which was rapidly cleared from the body, whilst that encapsulated into particles remained stable for prolonged periods of time in physiological environments. Besides, when the biodegradable nanoparticles were administered through the intravenous or intraperitoneal route, they were mostly accumulated in the spleen and liver for 24 h at least, showing an important retention of the nanoparticles in these two organs, with a remarkable stability of these probes. However, no important differences could be appreciated when studying the comparison of the biodistribution between the routes previously mentioned, indicating that the route of administration of the nanoparticles did not exert a significant modification on their *in vivo* organ distribution. By enabling the imaging in real time and *in vivo* biodistribution of these nanoparticles at high resolution in complete animals, optoacoustic imaging of DiR–PEI–PLGA nanocarriers allows unprecedented access to crucial information for accurate tailoring of delivery vehicles and their potential targeting to diseased tissue. This specific targeting could be obtained by functionalizing the nanoparticles with certain peptides or ligands that attach to receptors over-expressed in tumor cells. Furthermore, in order to increase the blood circulation time, avoiding the retention of the nanoparticles in the organs of the mononuclear phagocytic system (liver and spleen), hydrophilic polymers, such as PEG, can be attached to the surface of the nanoparticles (PEGylation). We foresee the immediate translation of this proof of concept study to preclinical studies of inflammatory and cancerous diseases, using passive as well as active targeting to drive the accumulation of the nanocarriers to the site of interest, ultimately enabling a simultaneous dual *diagnosis* (through targeting) and *therapy* (through nanocarrier accumulation and drug release) approach, dubbed *theranostics*, alongside access to pharmacological data in real time.

Acknowledgements

S.P.E. acknowledges support from the Basque Government (Gobierno Vasco, Departamento de Educación, Universidades e Investigación) for the fellowship research grant. This project was partially supported by the Ministerio de Economia y Competitividad for the subprogram INNPACTO (IPT-2012-0674-090000), FEDER funds and the Basque Government (Consolidated Groups, IT-407-07). N.B. and V.N. would like to thank the 'Nanosystem initiative Munich' Cluster of Excellence and the ERC advanced grant (233161) 'Next generation *in vivo* imaging platform for post-genome biology and medicine MSOT' for their financial support.

REFERENCES

1. Razansky D, Distel M, Vinegoni C, Ma R, Perrimon N, Koster RW, Ntziachristos V. Multispectral opto-acoustic tomography of deep-seated fluorescent proteins *in vivo*. Nat Photon 2009; 3(7): 412–417.
2. Ungureanu C, Van Weperen T, Sijl J, Rayavarapu R, Manohar S, Versluis M, Van Leeuwen TG. Acoustic signals from gold nanoparticles irradiated with pulsed lasers. J Acoust Soc Am 2008; 123(5): 3370.
3. Bao C, Beziere N, del Pino P, Pelaz B, Estrada G, Tian F, Ntziachristos V, de la Fuente JM, Cui D. Gold nanoprisms as optoacoustic signal nanoamplifiers for in vivo bioimaging of gastrointestinal cancers. Small 2013; 9(1): 68–74.
4. de la Zerda A, Zavaleta C, Keren S, Vaithilingam S, Bodapati S, Liu Z, Levi J, Ma T-J, Oralkan O, Cheng Z, Chen X, Dai H, Khuri-Yakub BT, Gambhir SS. Photoacoustic molecular imaging in living mice utilizing targeted carbon nanotubes. Nat Nanotechnol 2008; 3: 557–562.
5. Ntziachristos V, Razansky D. Molecular imaging by means of multispectral optoacoustic tomography (MSOT). Chem Rev 2010; 110(5): 2783–2794.
6. Lozano N, Al-Jamal WT, Taruttis A, Beziere N, Burton NC, Van den Bossche J, Mazza M, Herzog E, Ntziachristos V, Kostarelos K. Liposome–gold nanorod hybrids for high-resolution visualization deep in tissues. J Am Chem Soc 2012; 134(32): 13256–13258.
7. Yang Z, Leon J, Martin M, Harder JW, Zhang R, Liang D, Lu W, Tian M, Gelovani JG, Qiao A, Li C. Pharmacokinetics and biodistribution of near-infrared fluorescence polymeric nanoparticles. Nanotechnology 2009; 20(16): 165101.
8. Danhier F, Ansorena E, Silva JM, Coco R, Le Breton A, Préat V. PLGA-based nanoparticles: an overview of biomedical applications. J Control Release 2012; 161(2): 505–522.
9. Lu JM, Wang X, Marin-Muller C, Wang H, Lin PH, Yao Q, Chen C. Current advances in research and clinical applications of PLGA-based nanotechnology. Expert Rev Mol Diagn 2009; 9(4): 325–341.
10. Janib SM, Moses AS, MacKay JA. Imaging and drug delivery using theranostic nanoparticles. Adv Drug Deliv Rev 2010; 62(11): 1052–1063.
11. Altinoglu EI, Adair JH. Near infrared imaging with nanoparticles. Wiley Interdiscip Rev: Nanomed Nanobiotechnol 2010; 2(5): 461–477.
12. Kohl Y, Kaiser C, Bost W, Stracke F, Fournelle M, Wischke C, Thielecke H, Lendlein A, Kratz K, Lemor R. Preparation and biological evaluation of multifunctional PLGA-nanoparticles designed for photoacoustic imaging. Nanomedicine 2011; 7(2): 228–237.
13. Kohl Y, Kaiser C, Bost W, Stracke F, Thielecke H, Wischke C, Lendlein A, Kratz K, Lemor R. Near-infrared dye-loaded PLGA nanoparticles prepared by spray drying for photoacoustic applications. Int J Artif Organs 2011; 34(2): 249–252.
14. Wang H, Liu C, Gong X, Hu D, Lin R, Sheng Z, Zheng C, Yan M, Chen J, Cai L, Song L. *In vivo* photoacoustic molecular imaging of breast carcinoma with folate receptor-targeted indocyanine green nanoprobes. Nanoscale 2014; 6(23): 14270–14279.
15. Egusquiaguirre SP, Manguán-García C, Pintado-Berninches L, Iarriccio L, Carbajo D, Albericio F, Royo M, Pedraz JL, Hernández RM, Perona R, Igartua M. Development of surface modified biodegradable polymeric nanoparticles to deliver GSE24.2 peptide to cells: a promising approach for the treatment of defective telomerase disorders. Eur J Pharm Biopharm 2015; 91: 91–102.
16. Gutierro I, Hernandez RM, Igartua M, Gascon AR, Pedraz JL. Size dependent immune response after subcutaneous, oral and intranasal administration of BSA loaded nanospheres. Vaccine 2002; 21(1/2): 67–77.
17. Buehler A, Rosenthal A, Jetzfellner T, Dima A, Razansky D, Ntziachristos V. Model-based optoacoustic inversions with incomplete projection data. Med Phys 2011; 38(3): 1694–1704.
18. Vrignaud S, Benoit J, Saulnier P. Strategies for the nanoencapsulation of hydrophilic molecules in polymer-based nanoparticles. Biomaterials 2011; 32(33): 8593–8604.
19. Zheng C, Zheng M, Gong P, Jia D, Zhang P, Shi B, Sheng Z, Ma Y, Cai L. Indocyanine green-loaded biodegradable tumor targeting nanoprobes for in vitro and in vivo imaging. Biomaterials 2012; 33(22): 5603–5609.

SUPPORTING INFORMATION

Additional supporting information may be found in the online version of this article at the publisher's web site.